High Pressure Research: An International Journal

Publication details, including instructions for authors and subscription information:
http://www.tandfonline.com/loi/ghpr20

Phase transformations of the amorphous Zn-Sb alloy under high pressures

V. E. Antonov [a], O. I. Barkalov [a], M. Calvo-Dahlborg [b], U. Dahlborg [b], V. F. Fedotov [a], A. I. Harkunov [a], T. Hansen [c], E. G. Ponyatovsky [a] & M. Winzenick [d]

[a] Institute of Solid State Physics RAS, 142432, Chernogolovka, Moscow District, Russia

[b] LSG2M, CNRS UMR 7584, Ecole des Mines, Pare de Saurupt, 54042, Nancy, Cedex, France

[c] Institute Laue- Langevin, B.P. 156, F-38042, Grenoble, Cedex 9, France

[d] Fachbereich Physik, Universtat-GH-Paderborn, D-33095, Paderborn, Germany

Version of record first published: 01 Dec 2006.

To cite this article: V. E. Antonov, O. I. Barkalov, M. Calvo-Dahlborg, U. Dahlborg, V. F. Fedotov, A. I. Harkunov, T. Hansen, E. G. Ponyatovsky & M. Winzenick (2000): Phase transformations of the amorphous Zn-Sb alloy under high pressures, High Pressure Research: An International Journal, 17:3-6, 261-272

To link to this article: http://dx.doi.org/10.1080/08957950008245914

High Pressure Research, 2000, Vol. 17, pp. 261–272
Reprints available directly from the publisher
Photocopying permitted by license only

PHASE TRANSFORMATIONS OF THE AMORPHOUS Zn–Sb ALLOY UNDER HIGH PRESSURES

V. E. ANTONOV[a,*], O. I. BARKALOV[a], M. CALVO-DAHLBORG[b], U. DAHLBORG[b], V. F. FEDOTOV[a], A. I. HARKUNOV[a], T. HANSEN[c], E. G. PONYATOVSKY[a] and M. WINZENICK[d]

[a]*Institute of Solid State Physics RAS, 142432 Chernogolovka, Moscow District, Russia;* [b]*LSG2M, CNRS UMR 7584, Ecole des Mines, Parc de Saurupt, 54042 Nancy Cedex, France;* [c]*Institute Laue-Langevin, B.P. 156, F-38042 Grenoble Cedex 9, France;* [d]*Fachbereich Physik, Universtät-GH-Paderborn, D-33095 Paderborn, Germany*

(Received 1 October 1999)

Phase transformations occurring in initially amorphous $Zn_{41}Sb_{59}$ semiconductor at pressures to 10 GPa and temperatures to 350°C were studied using the measurement of electrical resistance, *in situ* energy dispersive X-ray diffraction and neutron diffraction on quenched high-pressure phases at ambient pressure. The studied $T-P$ region involves the regions of reversible and irreversible crystallisation and phase transitions between the equilibrium crystalline low-pressure and high-pressure phases.

Keywords: Amorphization; Pressure; X-ray diffraction; Neutron diffraction

1. INTRODUCTION

In the Zn–Sb system, a crystalline metallic δ-$Zn_{41}Sb_{59}$ phase with a yet undetermined crystal structure is formed at pressures above 7 GPa and temperatures above 250°C [1]. This phase can be retained at ambient pressure if previously quenched under a high pressure to

*Corresponding author. e-mail: antonov@issp.ac.ru

liquid nitrogen temperature. On heating at ambient pressure to room temperature, δ-$Zn_{41}Sb_{59}$ transforms to amorphous state, the am_1 phase [1, 2]. Placed under a high pressure again, the am_1 phase at room temperature undergoes a reversible first order phase transition to another amorphous phase, am_2, at about 1 GPa [3]. The am_2 phase transforms to a crystalline γ-$Zn_{41}Sb_{59}$ phase with a simple hexagonal lattice at about 6 GPa [4]. Phase transformations of initially amorphous $Zn_{41}Sb_{59}$ at elevated temperatures were studied within the $T-P$ region of 1 atm to 6 GPa and 17°C to 200°C [5]. This region involves the crystallisation line descending from 180°C at ambient pressure to 80°C at 5 GPa and the nearly vertical line of the $am_1 \leftrightarrow am_2$ transformation terminating in a critical point at about 100°C, see Figure 1.

In the present study of $Zn_{41}Sb_{59}$, the $T-P$ region is extended to 10 GPa and 350°C in order to include the line of the $\gamma \rightarrow \delta$ transition and the lines of transitions between the high-pressure δ-phase and the

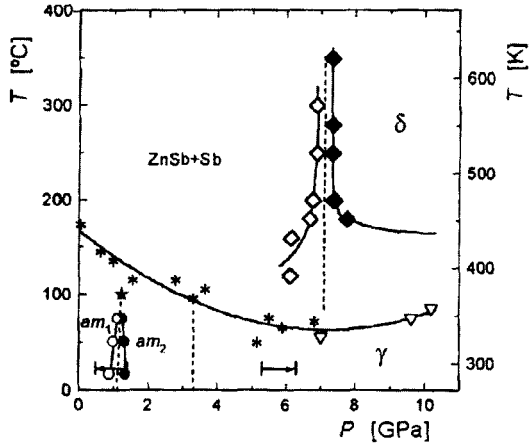

FIGURE 1 $T-P$ phase diagram for initially amorphous $Zn_{41}Sb_{59}$. am_1 and am_2 are the low- and high-pressure amorphous semiconductor phases, γ and δ are the high-pressure semi-metal and metal phase. The solid and open circles and diamonds indicate reversible transitions between corresponding states at increasing and decreasing pressure, respectively. The right and left arrows show the pressure intervals of the $am \rightarrow \gamma$ and $\gamma \rightarrow am$ transitions according to the X-ray data of Figure 3. The asterisks indicate the positions of the irreversible transitions of the *am* and γ phases to a mixture of ZnSb + Sb at increasing temperature; the open triangles indicate the irreversible $\gamma \rightarrow \delta$ transitions. The star marks the position of the critical point of the $am_1 \leftrightarrow am_2$ equilibrium line. The vertical dashed line at 3.3 GPa shows the tentative position of the line of the $am_2 \leftrightarrow \gamma$ metastable equilibrium.

mixture of ZnSb compound and antimony stable at low pressures. The transition lines are constructed using the electrical resistance measurement. The crystal structures of the γ-phase and δ-phase are examined by X-ray diffraction at high pressures using a diamond anvil cell and synchrotron radiation. The structure of the quenched δ-phase is also studied by neutron diffraction at ambient pressure and 100 K using samples made of Sb alloyed with Zn of the natural isotopic composition and with ^{67}Zn isotope.

2. EXPERIMENTAL

A pellet of amorphous $Zn_{41}Sb_{59}$ 7.5 mm in diameter and 3 mm thick was prepared by the same procedure as previously [5]. The electrical resistance was measured with the samples 5–8 mm long and 1 × 1 mm across cut from this pellet. The sample was placed in a Toroid-type high-pressure chamber using hexagonal BN as pressure transmitting medium and the resistance was measured by a d. c. four-probe method with copper electrodes pressed against the sample. The temperature and pressure were determined accurate to within ± 7°C and ± 0.3 GPa, respectively.

Energy dispersive X-ray diffraction (EDXD) was performed with synchrotron radiation and diamond anvil cells in HASYLAB at DESY, Hamburg. A piece from a pellet of amorphous $Zn_{41}Sb_{59}$ of nearly 150 μm diameter and around 20 μm thickness was loaded with white mineral oil and a few ruby grains into the central hole of the Inconel gasket [6]. The spectra were recorded by a Ge detector over periods of 10 min in the course of the step-wise changes in pressure, which was measured by the ruby luminescence technique with an accuracy of ± 0.1 GPa. The diffraction angle was $2\vartheta = 9.7174°$ or 11.5666° for minimum overlap of the antimony fluorescence lines with the diffraction halos of the amorphous phases and with the diffraction lines of the crystalline phases, respectively.

The samples of the δ-phase with natural Zn and with ^{67}Zn were studied by neutron diffraction at 100 K with neutrons of a wavelength of $\lambda = 2.41$ Å using the D20 instrument at the ILL, Grenoble. The samples weighing about 1 g each were produced by exposing powdered and pelletised mixture of ZnSb and Sb to 8 GPa and 325°C for 24 h.

The background was determined in a separate empty-can measurement and subtracted from the measured diffraction patterns.

3. RESULTS AND DISCUSSION

Figure 1 presents the $T-P$ diagram of $Zn_{41}Sb_{59}$ that combines the data of Ref. [5] and the present work. Figure 2 shows representative dependences of the electrical resistance used in the present work to construct the lines of transitions involving the δ-phase.

To measure the $\rho(P)$ isotherms in the region of the $ZnSb+Sb \leftrightarrow \delta$ transformation (Fig. 2a), the amorphous $Zn_{41}Sb_{59}$ samples were first crystallised to a mixture of ZnSb+Sb by heating at a low pressure. According to the phase rule, the transition between the thermodynamically equilibrium two-phase ZnSb+Sb state and single δ state should be a complex multi-step process. However, judging by the presence of only one step in the $\rho(P)$ isotherms, the pressure intervals of the intermediate transitions significantly overlap. Therefore, only midpoints of the steps in the $\rho(P)$ dependences were plotted in Figure 1.

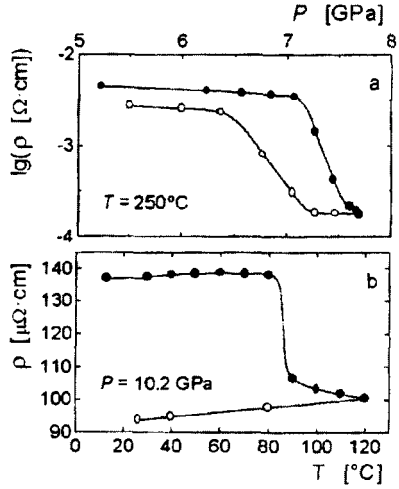

FIGURE 2 The isotherms (a) and isobars (b) of the electrical resistivity, ρ, of $Zn4_1Sb_{59}$ measured on a step-wise increase (solid circles) and decrease (open circles) in pressure and temperature, respectively.

The midpoints of the steps in the $\rho(T)$ isobars (Fig. 2b) measured at increasing temperature were taken as the temperatures of crystallisation of amorphous $Zn_{41}Sb_{59}$. The product of crystallisation, either the δ-phase or a ZnSb + Sb mixture at lower pressures, was identified by X-ray diffraction on quenched samples at ambient pressure (DRON-2.0 diffractometer, CuK_α radiation, 100 K). The results agree with the position of the ZnSb + Sb $\leftrightarrow$ δ equilibrium line at $P = 7.1$ GPa shown by the vertical dashed line in Figure 1.

The elements of the $T-P$ diagram positioned below the crystallisation line in Figure 1 refer to metastable equilibria between the phases with one and the same composition $Zn_{41}Sb_{59}$. Figure 3 presents the room-temperature X-ray patterns demonstrating a reversible transformation between the crystalline γ-phase and the amorphous phase characterised by two broad diffraction halos. Partial crystallisation of the am_2-phase to the equilibrium ZnSb + Sb mixture occurred at pressures of 5 to 6 GPa because of the too slow pressure increase in this pressure interval where the amorphous state is most thermally unstable. No such crystallisation was observed in other our experiments. The label 'ZnSb + Sb' in Figure 3 marks the peak composed of the strongest diffraction lines of ZnSb and Sb.

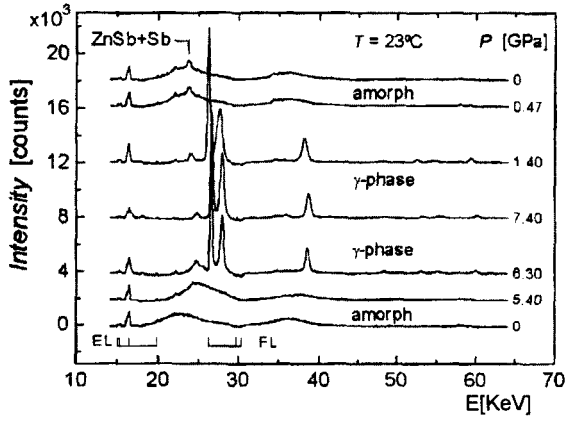

FIGURE 3 The EDXD spectra of the initially amorphous $Zn_{41}Sb_{59}$ alloy measured at room temperature and different pressures in the course of a step-wise pressure increase and further decrease (the sequence is from the bottom of the figure upwards) using a diffraction angle of $2\vartheta = 9.7174°$. The fluorescence lines have been subtracted; their positions (FL) and the positions of the escape lines (EL) are indicated with solid vertical bars.

In agreement with Ref. [4], diffraction patterns of the γ-phase can be indexed with a simple hexagonal cell, space group $P6$ (No. 168). As seen from Figure 4, the cell parameters vary with pressure approximately linearly. Their values at 8 GPa are $a_{hex} = 3.018$ Å and $c_{hex} = 2.742$ Å. Linear extrapolation to ambient pressure gives $a_{hex} = 3.068$ Å, $c_{hex} = 2.793$ Å and the atomic volume $V_a = 22.76$ Å^3/atom; the compressibility is $æ_\gamma = -(1/V_a)(\partial V_a/\partial P) = 0.0069$ GPa^{-1}. For comparison: the atomic volume of the am_1-phase under ambient conditions is 27.2 Å^3/atom [5], $æ_{am1} = 0.026$ GPa^{-1}, $æ_{am2} = 0.016$ GPa^{-1} and the volume decrease accompanying the $am_1 \rightarrow am_2$ transition at room temperature is 0.8% [3]. The volume effect of the $am_2 \leftrightarrow \gamma$ transformation calculated using these data is about 12% at a pressure of 3.3 GPa, the centre of the hysteresis interval of the $am_2 \leftrightarrow \gamma$ transformation at room temperature. The effect is large and therefore the slope of the line of the $am_2 \leftrightarrow \gamma$ metastable equilibrium must also be large according to Clapeyron equation. This line is schematically shown in Figure 1 by the vertical dashed line erected at 3.3 GPa.

Relative intensities and widths of diffraction lines of the γ-phase were well reproduced in 5 our EDXD experiments with different pieces of the initial amorphous $Zn_{41}Sb_{59}$. This suggests the small grain size and the absence of significant texture in the samples. However, as seen

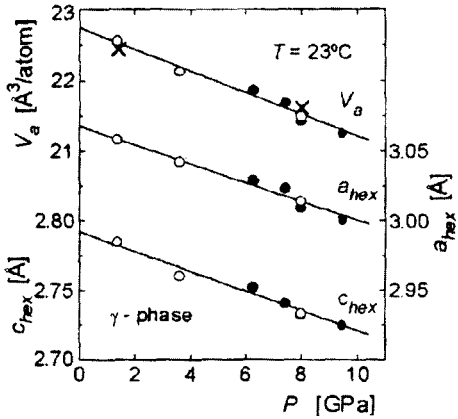

FIGURE 4 The lattice parameters, a_{hex} and c_{hex}, of the simple hexagonal cell and the atomic volume $V_a = (\sqrt{3}/2)a_{hex}^2 c_{hex}$ for the γ-phase as a function of increasing (solid circles) and decreasing (open circles) pressure at room temperature. The crosses show the atomic volumes $V_a = a_{orth} b_{orth} c_{orth}/2$ of the δ-phase with an orthorhombic pseudo-cell.

from Figure 5, the experimental intensities strongly differ from those calculated for the simple hexagonal cell. In particular, the integral intensities of the (001), (002) and (102) lines are much higher than calculated. For instance, the experimental intensity ratio for the (001) and (100) peaks is about 2:1 instead of the calculated 1:3. Additionally, the width of the (001) line is by about 1.5 times smaller than the width of the (100) line.

The above peculiarities in the X-ray patterns of the γ-phase can be ascribed to chaotic static displacements of Zn and Sb atoms in the (001) planes, the arrangement of these planes along the z-axis remaining periodical. The resulting disc-like clouds of displacements are schematically shown in Figure 6 and can be modelled in the framework of the space group $P6$ by displacing some atoms from the position $1a$ (0,0,0) of the simple hexagonal structure to the position $6d$ $(x, x, 0)$. With $x = 1/3$, a satisfactory profile fit of the experimental EDXD spectra of the γ-phase can be achieved with about 35% atoms on the $6d$ sites, irrespective of the pressure applied.

In one EDXD experiment, the $Zn_{41}Sb_{59}$ sample was heated to 100°C at $P = 8$ GPa for 2 h in order to transform it to the δ-state and then cooled and studied at room temperature. As can be seen from comparison of curves (a) and (b) in Figure 7, the positions and relative intensities of the first three strong lines of the δ-phase did not differ

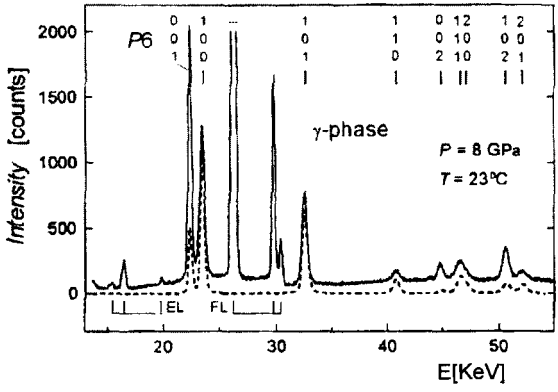

FIGURE 5 The EDXD spectrum of γ-$Zn_{41}Sb_{59}$ at $P = 8$ GPa and $2\vartheta = 11.5666°$ (solid line) and the calculated profile for the phase with the simple hexagonal lattice (dashed line).

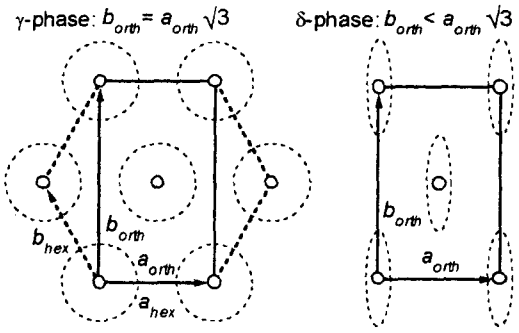

FIGURE 6 Schematic plots of the (001) planes in the unit cells of the γ- and δ-phase formed at high pressures at room temperature. The dashed circles and ellipses illustrate the symmetry of distribution of static displacements of atoms in these planes. a_{hex} and b_{hex} are the parameters of the simple hexagonal cell, a_{orth} and b_{orth} of the orthorhombic cells.

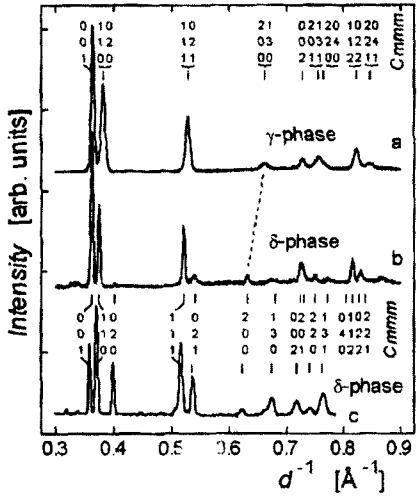

FIGURE 7 The EDXD spectra of the γ-phase (a) and δ-phase (b) measured at a pressure of 8 GPa and room temperature using a diffraction angle of $2\vartheta = 11.5666°$, and the neutron diffraction spectrum of the quenched δ-phase (c) measured at ambient pressure and 100 K. The *x*-axis is in units of reciprocal inter-planar distances d^{-1}. The spectrum of the simple hexagonal γ-phase, curve (a), is indexed based on an orthorhombic unit cell for easier comparison with the spectra of the δ-phase.

much from those of the γ-phase, so the structures of these phases should be closely related. At the same time, the widths of the first three intensive peaks of curve (b) are by about 1.5 times smaller than in

curve (a), the positions of the fourth intensive peaks of these curves, connected with the dashed line in Figure 7, are significantly different and curve (b) contains new weak lines. This suggests a higher degree of order and a lower symmetry of the crystal structure of the δ-phase.

The structure of the δ-phase is too complex to be determined in full from powder diffraction data. However, as seen from Figure 7, the main peaks in the EDXD spectrum of the δ-phase can be indexed with a rather small base-centred orthorhombic cell, space group *Cmmm* (No. 65). The parameters of the cell at room temperature are $a_{orth}/b_{orth}/c_{orth} = 3.156/4.971/2.757$ Å at $P = 8$ GPa and 3.206/5.017/2.791 Å at $P = 1.4$ GPa. The corresponding values of atomic volumes are indicated in Figure 4 by crosses. Within the experimental error they coincide with those of the γ-phase at the same pressures.

The simple hexagonal structure of the γ-phase can be formally represented using a base-centred orthorhombic cell with the x- and y-axis chosen as shown in Figure 6 and the ratio of $b_{orth}/a_{orth} = \sqrt{3}$. For the γ-phase at 8 GPa this gives $a_{orth}/b_{orth}/c_{orth} = 3.018/5.227/2.742$ Å. Comparison with the data for the δ-phase at this pressure shows that the $\gamma \rightarrow \delta$ transition is accompanied by an increase in a_{orth} and a decrease in b_{orth}, while the value of c_{orth} changes only slightly. The ratio of b_{orth}/a_{orth} decreases to $\sqrt{2.481}$ that effectively lifts the 'degeneracy' of the diffraction lines in the spectrum of the γ-phase resulting from their indexing with an orthorhombic unit cell, compare curves (a) and (b) in Figure 7.

Analysis of the line intensities shows that the δ-phase partly inherited the defect structure of the γ-phase. In the EDXD spectrum of the δ-phase, the lines with a large index k, such as (020), (021), (130) and (131), have much lower intensities than calculated for the defect-free orthorhombic structure. This can be ascribed to chaotic static displacements of Zn and Sb atoms predominantly along the y-axis. As schematically shown in Figure 6, the disc-like clouds of atomic displacements in the γ-phase thus transform to the anisotropic ellipse-like clouds in the δ-phase. In the framework of the space group *Cmmm*, the latter can be modelled by displacing some atoms from the position 2*a* (0,0,0) to 8*p* $(x, y, 0)$. With $x = 0.1$ and $y = 1/4$, about 35% atoms should be placed on the 8*p* sites to describe qualitatively the intensities of the main diffraction lines of the δ-phase.

The γ-phase seems to be a highly metastable state of the $Zn_{41}Sb_{59}$ alloy and at $P = 1$ atm it gets amorphous at temperatures below 100 K. Noticeable amorphization of the δ-phase at ambient pressure begins only on heating above 170 K [3]. Two quenched samples of the δ-phase were studied in the present work by neutron diffraction (ND) at ambient pressure and 100 K. The results are presented in Figures 7 and 8.

The ND pattern of the quenched δ-phase contained the same set of diffraction lines as the EDXD pattern, compare curves (b) and (c) in Figure 7, but the intensities of the main lines were changed drastically and the intensities of the additional lines were significantly higher. As seen from Figure 8, the intensities of the main lines of the quenched δ-phase can be satisfactorily described with the defect-free orthorhombic unit cell. This corroborates the interpretation of the line intensities in the EDXD spectra of the δ-phase as being strongly affected by lattice defects: The quenched sample was prepared at higher temperature (325°C instead of 100°C) and exposed to this temperature for a longer time (24 h *vs.* 2 h) that should have lead to a better annealing of defects.

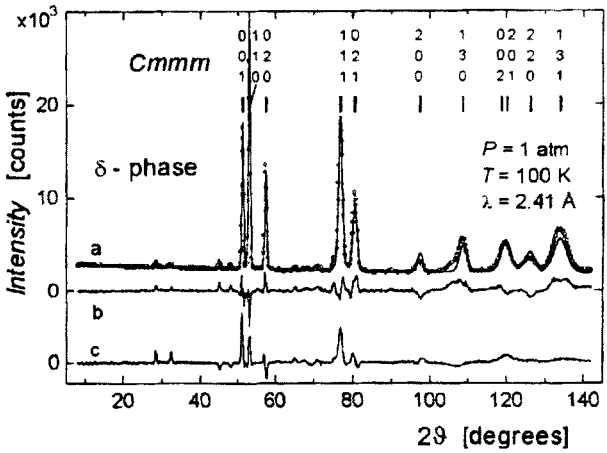

FIGURE 8 The neutron diffraction spectrum of the quenched δ-$Zn_{41}Sb_{59}$ sample measured at ambient pressure and 100 K (dots), the profile fit of the main peaks of this spectrum shown by the solid line (a) and the difference between the experimental and calculated spectrum (b). Curve (c) is the difference between the experimental spectra of the δ-phase with natural Zn (dots) and with ^{67}Zn isotope. For both samples $a_{orth}/b_{orth}/c_{orth} = 3.205/5.016/2.790$ Å.

The high-pressure phases of $Zn_{41}Sb_{59}$ belong to a family of Hume–Rothery phases usually exhibiting no chemical order. Nevertheless, the investigation of the quenched samples of the δ-phase with natural Zn and with ^{67}Zn isotope revealed significant differences in their ND patterns (curve (c) in Fig. 8) that is possible only for chemically ordered structures.

Furthermore, the neutron scattering lengths of antimony and zinc do not differ much: $b_{Sb} = 5.57$ fm, $b_{Zn} = 5.69$ fm, $b_{Zn\text{-}67} = 7.59$ fm [7]. The difference between the scattering lengths of Zn and ^{67}Zn is too little for the strong isotopic dependence of the intensities of the main lines (001), (110) and (111) can be ascribed to any ordered arrangement of Sb and Zn atoms over crystallographically equivalent sites. The process of chemical ordering in δ-$Zn_{41}Sb_{59}$ therefore must be accompanied by significant displacements of the atoms from their positions in the base-centred orthorhombic lattice and the unit cell of the ordered structure is large and has lower symmetry. Note, that complex crystal structures are characteristic of low-pressure Zn–Sb phases as well [8].

Acknowledgements

This work was supported by the Grants Nos. 99-02-17007 and 96-15-96806 from the Russian Foundation for Basic Research, by the Grant No. 34-1997 for young scientists from the Russian Academy of Sciences and by the Project No. 4069 of CNRS-RAS collaboration. One of the authors (OIB) thanks the Alexander von Humboldt Foundation for a Research Fellowship and thanks HASYLAB for financial support and the hospitality during his stay at DESY, Hamburg. Financial support by the German Ministry of Research and Technology under contract No. 05647PPA is gratefully acknowledged. The authors are grateful to Prof. W. B. Holzapfel for helpful discussions and would like to thank W. Bröckling for technical assistance.

References

[1] Belash, I. T. and Ponyatovsky, E. G. (1977). *High Temp.–High Press.*, **9**, 651.
[2] Belash, I. T., Degtyareva, V. F., Ponyatovskii, E. G. and Rashchupkin, V. I. (1987). *Sov. Phys. Solid State*, **29**, 1028.

[3] Antonov, V. E., Arakelyan, A. E., Barkalov, O. I., Gurov, A. F., Ponyatovsky, E. G., Rashupkin, V. I. and Teplinsky, V. M. (1993). *J. Alloys Compds.*, **194**, 279.
[4] Degtyareva, V. F., Bdikin, I. K. and Khasanov, S. S. (1997). *Sov. Phys. Solid State*, **39**, 1341.
[5] Antonov, V. E., Barkalov, O. I., Fedotov, V. K., Harkunov, A. I., Kolyubakin, A. I., Ponyatovsky, E. G. and Winzenick, M., *Phys. Rev. B*, in press.
[6] Holzapfel, W. B. (1978). In: *High Pressure Chemistry*, Kelm, H. (Ed.). [Reidel, Boston], p. 177.
[7] Koester, L., Rauch, H. and Seymann, E. (1991). *Atomic Data and Nuclear Data Tables*, **49**, 65.
[8] Hansen, M. and Anderko, K. (1958). *Constitution of Binary Alloys* [McGraw-Hill, New York].